Chin. J. Mech. Eng. (2017) 30:943–950
DOI 10.1007/s10033-017-0110-8

ORIGINAL ARTICLE

Energy Expenditure of Trotting Gait Under Different Gait Parameters

Xian-Bao Chen[1] · **Feng Gao**[1]

Received: 7 December 2016 / Revised: 3 January 2017 / Accepted: 12 January 2017 / Published online: 17 May 2017

Abstract Robots driven by batteries are clean, quiet, and can work indoors or in space. However, the battery endurance is a great problem. A new gait parameter design energy saving strategy to extend the working hours of the quadruped robot is proposed. A dynamic model of the robot is established to estimate and analyze the energy expenditures during trotting. Given a trotting speed, optimal stride frequency and stride length can minimize the energy expenditure. However, the relationship between the speed and the optimal gait parameters is nonlinear, which is difficult for practical application. Therefore, a simplified gait parameter design method for energy saving is proposed. A critical trotting speed of the quadruped robot is found and can be used to decide the gait parameters. When the robot is travelling lower than this speed, it is better to keep a constant stride length and change the cycle period. When the robot is travelling higher than this speed, it is better to keep a constant cycle period and change the stride length. Simulations and experiments on the quadruped robot show that by using the proposed gait parameter design approach, the energy expenditure can be reduced by about 54% compared with the 100 mm stride length under 500 mm/s speed. In general, an energy expenditure model based on the gait parameter of the quadruped robot is built and the trotting gait parameters design approach for energy saving is proposed.

Supported by National Basic Research Program of China (973 Program, Grant No. 2013CB035501).

✉ Feng Gao
fengg@sjtu.edu.cn

[1] State Key Laboratory of Mechanical System and Vibration, Shanghai Jiao Tong University, Shanghai 200240, China

Keywords Quadruped robot · Energy expenditure · Gait · Bezier curve

1 Introduction

With the development of robot technology, more robots are able to walk outside the lab autonomously. Combustion robots can carry fuel by themselves and travel for a long distance [1–4]. In many cases however, a combustion engine is not the first choice due to the heat, vibration and exhaust emission; especially when the robot is working indoors or in space (such as on the moon), battery is a better option [5–9]. The electrical motor powered by battery is clean, quiet and its control system is stable and mature. But battery endurance is still a great challenge. The energy density of batteries is two orders of magnitude below that of liquid fuels [10, 11]. Increasing the number of battery cells may help, but too many become a great burden and reduce the power to weight ratio of the robot. In order to extend the working hours, many energy saving strategies can be applied. The most common method is to use springs to store and release energy during walking [12, 13]. GREGORIO et al. [14] and ACKERMAN et al. [15], proposed serial spring configuration designs to save energy. CHEN et al. [16], proposed a parallel configured spring method that can efficiently reduce energy consumption for a hydraulic quadruped robot.

Besides the springs, walking pattern is another critical influence on the energy expenditure. ALEXANDER [17] studied the energy saving mechanisms in walking and running. HOYT et al. [18, 19], discussed the relation between gait parameters and energetics in terrestrial locomotion. MINETTI et al. [20], discovered the relationship between mechanical work and energy expenditure of

locomotion on horses. Legged animals can freely choose locomotion speed and gaits to save their physical energy. But legged robots can only be controlled by the operator and the speed is determined according to different tasks.

Resonant locomotion is an attractive theory about energy efficiency. CAVAGNA et al. [21], studied the effects of the natural frequency of the bouncing system in the stance phase. HOLT et al. [22], suggested that the preferred stride frequency(PSF) of human walking was predictable using the resonant frequency of a force-drive harmonic oscillator (FDHO). The model is related to the swing phase. Later he proposed another model [23] called the hybrid pendulum-spring model to consider both the swing phase and the stance phase. AHLBORN et al. [24], gave another method to predict the frequency. However, the resonant frequency might be too fast or too slow for some robots under a certain travelling speed.

This paper not only intends to discuss how the stride frequency and stride length under a given trotting speed affect the energy expenditure of the quadruped robot, but also aims to determine these parameters automatically. Firstly, the robot models are built and the mechanical works in the swing phase and the stance phase are analyzed. The optimal gait parameters under a given speed are found. No matter whether the robot can trot in the resonant frequency or not, there still exists optimal gait parameters. Secondly, when the mechanical work in a unit distance under different trotting speeds is studied, a critical trotting speed is discovered and used to determine the gait parameters. When the robot is travelling lower than this speed, it is better to keep a constant stride length and change the cycle period. When the robot is travelling higher than this speed, it is better to keep a constant cycle period and change the stride length. Finally, simulations and the experiments reveal that these parameters have a great influence on the energy expenditure.

This paper is organized in six sections. In Sect. 2, the robot leg and its gait planning procedure will be briefly introduced. Section 3 will discuss the modelling of the robot. The energy expenditure analysis and the gait parameters design approach will be introduced in Sect. 4, and the effects are presented by simulations and experiments in Sect. 5. Concluding remarks are given in Sect. 6.

2 Leg Mechanism and Gait Planning

The theory is implemented on a quadrupe d robot called the Baby Elephant [25–28] shown in Fig. 1. The robot uses a hybrid leg mechanism. In the sagittal plane, it is a parallel mechanism. Each cylinder drives one linkage connecting to the hip joint. The side movement is controlled by another hydraulic cylinder alone.

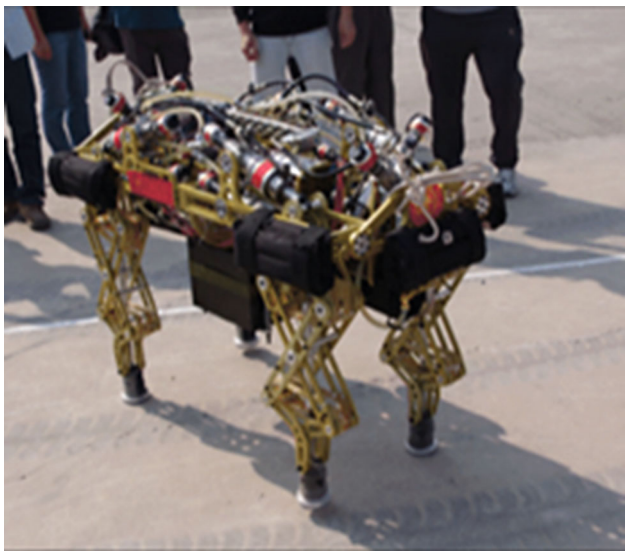

Fig. 1 Mechanical structure of the robot

As shown in Fig. 2 the origin of the leg frame is set at the hip joint. Given the position of the foot tip P, the length of the left and that of right cylinder are expressed in Eq. (1):

$$\begin{aligned} q_r^2 &= x_r^2 + z_r^2 + r^2 - 2r\sqrt{x_r + z_r}\cos(\lambda_r + \gamma_r), \\ q_l^2 &= x_l^2 + z_l^2 + r^2 - 2r\sqrt{x_l + z_l}\cos(\lambda_l + \pi - \gamma_l). \end{aligned} \tag{1}$$

During trotting, the robot can be regarded as an inverted pendulum with a prismatic joint along the stretch direction as shown in Fig. 3.

If the height of the body doesn't change during trotting, the dynamic model of the robot can be simply expressed as follows:

$$M\ddot{x} = f\sin\theta = \frac{Mg}{\cos\theta}\sin\theta, \tag{2}$$

where M is the body mass, f is the contact force through the center of mass, θ is the swing angle of the leg. Solving Eq. (2) obtains the motion of the body as follows:

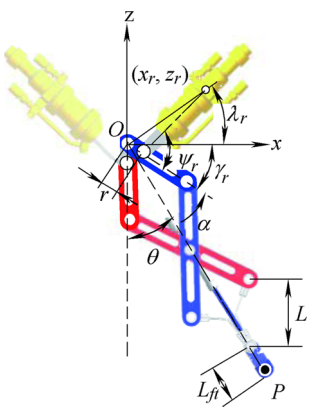

Fig. 2 Mechanism in the sagittal plane

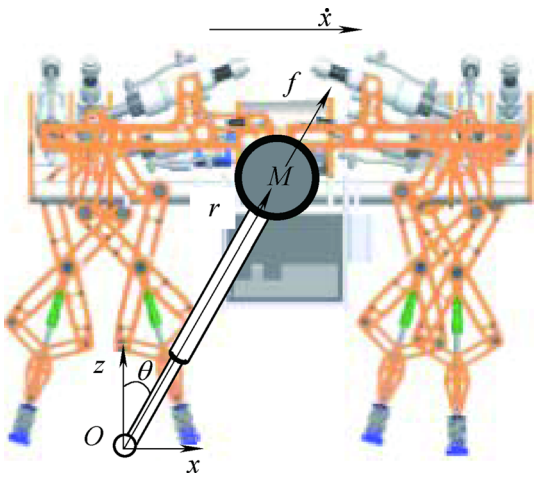

Fig. 3 Invert pendulum model of trotting gait

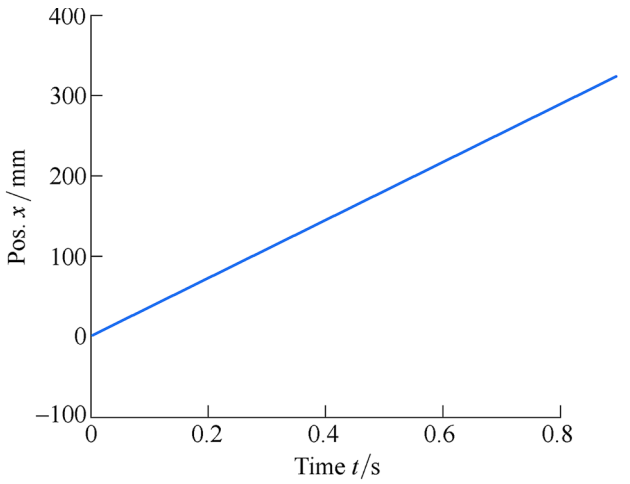

(a) Body trajectory

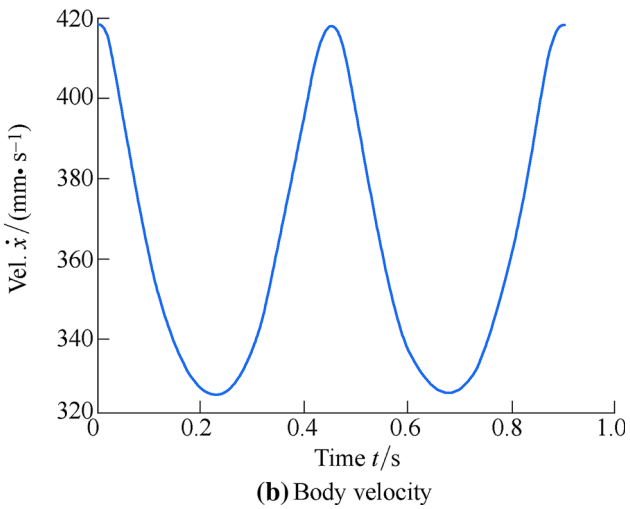

(b) Body velocity

Fig. 4 Body trajectory and body velocity during trotting

$$x(t) = x(0)\cosh\left(\frac{t}{T_c}\right) + T_c\dot{x}(0)\sinh\left(\frac{t}{T_c}\right), \tag{3}$$

$$\dot{x}(t) = \frac{x(0)}{T_c}\sinh\left(\frac{t}{T_c}\right) + \dot{x}(0)\cosh\left(\frac{t}{T_c}\right), \tag{4}$$

where

$$T_c = \sqrt{\frac{z}{g}}$$

$$\cosh\left(\frac{t}{T_c}\right) = \frac{\exp\left(\frac{t}{T_c}\right) + \exp\left(-\frac{t}{T_c}\right)}{2}$$

$$\sinh\left(\frac{t}{T_c}\right) = \frac{\exp\left(\frac{t}{T_c}\right) - \exp\left(-\frac{t}{T_c}\right)}{2}.$$

Figure 4 shows the motion of the robot body in the x direction. It can be seen that the robot is not moving in a constant velocity.

$$\begin{aligned} B(t) = {} & c_0(1-t)^5 + 5c_1(1-t)^4 t + 10c_2(1-t)^3 t^2 \\ & + 10c_3(1-t)^2 t^3 + 5c_4(1-t)t^4 + c_5 t^5. \end{aligned} \tag{5}$$

$$\begin{pmatrix} c_0 \\ c_1 \\ c_2 \\ c_3 \\ c_4 \\ c_5 \\ c_6 \end{pmatrix} = \begin{pmatrix} x_s \\ \frac{T_{sp}\dot{x}_s + 5x_s}{5} \\ \frac{20x_s + T_{sp}^2\ddot{x}_s + 8T_{sp}\dot{x}_e}{20} \\ \frac{20x_e + T_{sp}^2\ddot{x}_e - 8T_{sp}\dot{x}_e}{20} \\ \frac{-T_{sp}\dot{x}_e + 5x_e}{5} \\ \dot{x}_e \end{pmatrix}, \tag{6}$$

where T_{sp} is the cycle period of the curve.

Equation (5) is the expression of a fifth order Bezier curve. It is the same as an ordinary polynomial curve. Giving the positions (x_s, x_e), velocities $(\dot{x}_s, \dot{x}_e)$ and accelerations $(\ddot{x}_s, \ddot{x}_e)$ at the beginning point and the ending point, the coefficients of the curve can be expressed.

To compute the coefficients of an ordinary polynomial curve, matrix inversion is needed. The advantage of using the Bezier curve is that the coefficients can be explicitly expressed as shown in Eq. (6). Thus, the computing speed can be efficiently increased. Combining the stance phase and the swing phase, the trajectories of the foot tips are plotted in Fig. 5.

3 Modelling of the Robot Leg

There are two phases in trotting: the stance phase and the swing phase. In the stance phase, the leg can be modeled as an inverted pendulum with half of the body mass M' at the

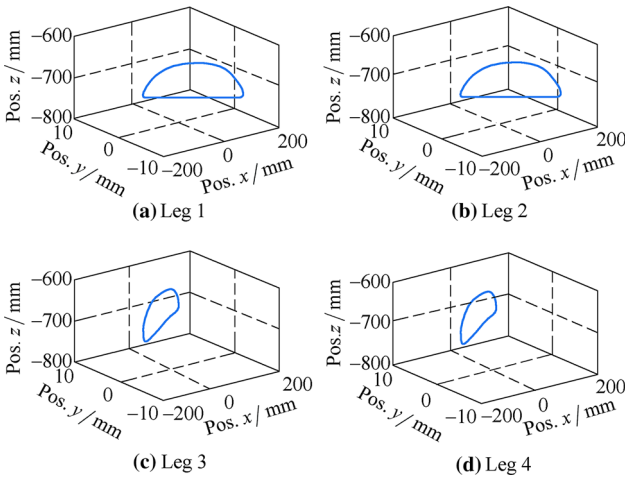

Fig. 5 Trajectories of foot tips for trotting gait

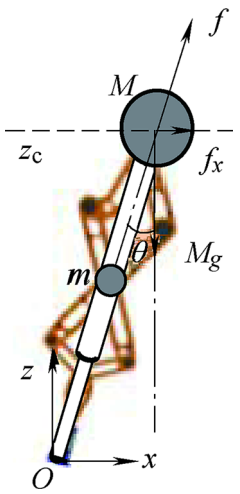

Fig. 6 Leg model in the stance phase

mass center as shown in Fig. 6. This is because two legs are supporting the body in trotting.

According to the gait trajectories, the mechanical work is mostly used to push the body in the horizontal direction. In this phase, the leg moment of inertia can be ignored and its mass is added to the mass center M'. So the mechanical work from the touchdown position to the neutral position can be expressed as

$$W_{\text{td2m}} = \int_{t=0}^{\beta T/2} f_x(t)\dot{x}(t)\mathrm{d}t, \tag{7}$$

where β is the duty factor and T is the cycle period of the gait. Substituting Eq. (2) into Eq. (7) obtains

$$W_{\text{td2mid}} = \frac{M'g}{z}\int_{t=0}^{\beta T/2} \dot{x}(t)x(t)\mathrm{d}t. \tag{8}$$

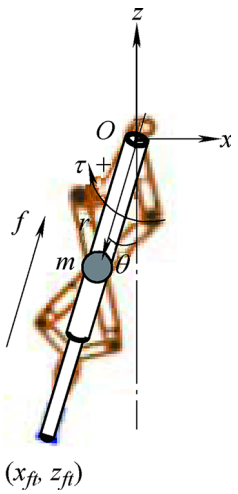

Fig. 7 Leg model in the swing phase

Equation (8) can be rewritten as follows:

$$W_{\text{td2mid}} = \frac{M'gL_{\text{B}}^2}{8z}, \tag{9}$$

where L_{B} is the stride length in the body frame. In order to focus on the effect of the gait parameters, the springs at the foot tips are not discussed. Therefore, the energy expenditure in the stance phase is twice as much as W_{td2mid}. It can be expressed in

$$W_{\text{td}} = \frac{M'gL_{\text{B}}^2}{4|z|}. \tag{10}$$

It can be seen that for a given body height z, larger stride length leads to larger energy consumption in the stance phase.

In the swing phase, if the stride frequency is high, the mass and the moment of inertia can no longer be ignored. As shown in Fig. 7, the leg can be modelled as a simple physical pendulum with its length stretchable. Its dynamic model can be expressed in Eqs. (11) and (12):

$$m\ddot{r} + mr_{\text{m}}\dot{\theta}^2 + mg\cos\theta + m\ddot{x}\sin\theta = f \tag{11}$$

$$I\ddot{\theta} - 2mr_{\text{m}}\dot{r}\dot{\theta} + mgr_{\text{m}}\sin\theta + m\ddot{x}r_{\text{m}}\cos\theta = \tau \tag{12}$$

where r_{m} represents the distance from the mass center to the rotating center, I represents the moment of inertia, m is the leg mass and τ is the equivalent torque to the rotating center.

The moment of inertia of the pendulum can be expressed in

$$I = \frac{mr^2}{3}. \tag{13}$$

The moment of inertia of the robot leg can be calculated in

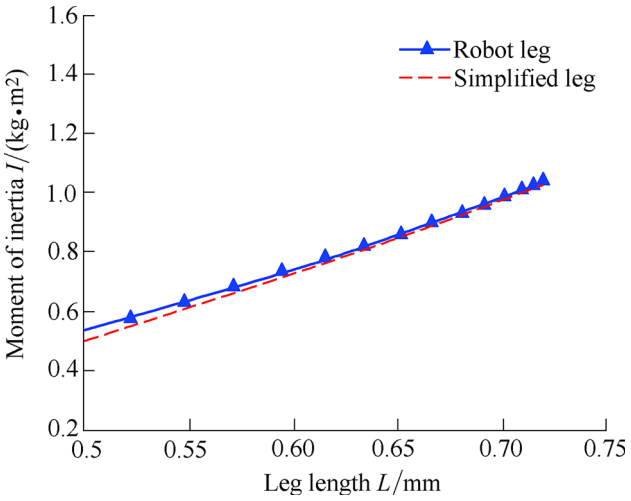

Fig. 8 Leg moment of inertia

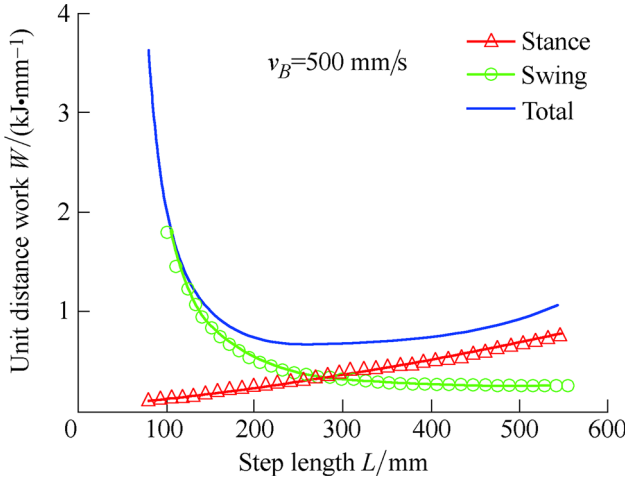

Fig. 9 Energy expenditure of a certain speed under different parameters

$$I_p = \frac{8}{3} m_{\text{link}} L^2 + 40 m_{\text{link}} L^2 \cos^2 \alpha, \tag{14}$$

where m_{link} is the mass of the link.

Substituting the parameters into Eqs. (13) and (14) obtains the curves shown in Fig. 8. It can be seen that the pendulum leg model makes little difference to the robot leg.

Multiply by $\dot{r}$ on both side of Eq. (11) and $\dot{\theta}$ on both sides of Eq. (12), add them up and then take the integral. The mechanical work in the swing phase can be expressed as follows:

$$W_{\text{sw}} = \int_{t=0}^{T} \left(f\dot{r} + \tau\dot{\theta} \right) \mathrm{d}t. \tag{15}$$

According to the foot tip trajectories mentioned above in Eq. (5), the value of the mechanical work of the robot can

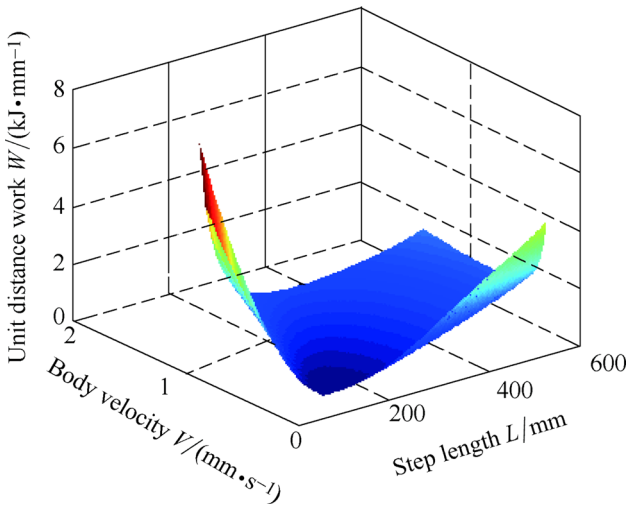

Fig. 10 Energy expenditure surface of trotting

be obtained. For convenience, the energy expenditure can be expressed as the mechanical work in a unit of distance which the robot traverses. The expression is shown as follows:

$$W_{\text{per\_dist}} = 2\beta \frac{W_{\text{sw}} + W_{\text{td}}}{L_{\text{B}}}, \tag{16}$$

where β is the duty factor of the gait.

4 Energy Expenditure Analysis and Gait Parameters Design

By substituting the parameters of the real robot into the Eq. (16), the energy expenditure within a gait cycle can be computed. As shown in Fig. 9, the curve with triangles stands for the energy expenditure of the stance legs. It is proportional to the step length. The curve with circles represents the energy expenditure of the swing legs. For a given speed, the energy cost grows rapidly as the step length is close to zero. The solid curve represents the sum of the two curves. It represents the mechanical work of the robot when it goes through a unit distance. It can be seen that there is a minimum value on the curve.

Figure 9 is a cross section of a certain speed. It proves the existence of the optimal gait parameters which can minimize the energy expenditure. Figure 10 shows the energy expenditure surface. There are two peak values for a given range of speed. The first appears when the robot is moving fast but the step length is very small. The second one appears when the step length is very large but the robot is moving slowly. The results reflect common sense.

By finding the minimum energy expenditure value for different trotting speeds, the optimal gait parameter curves are obtained as shown in Fig. 11. The dash curve stands for

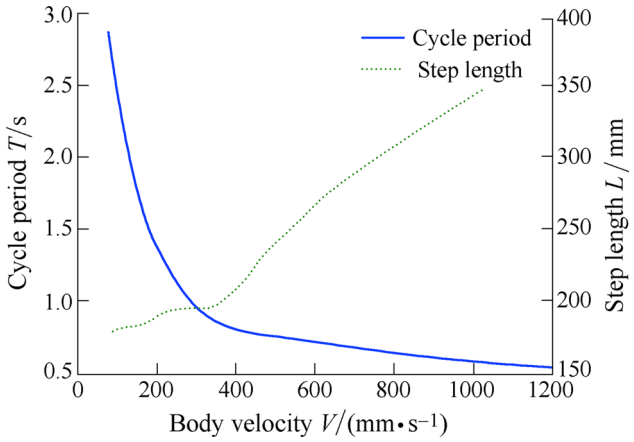

Fig. 11 Influence of gait parameters to energy expenditure

Fig. 12 Simulations of the trotting gait

the step length. The solid curve stands for the cycle period calculated from the corresponding body velocity and step length. For a given trotting speed, the optimal gait parameters can be found using these curves. However, the relationship between the speed and the optimal gait parameters is nonlinear, which is difficult for practical application.

It is interesting to see that there is a critical speed value about 300 mm/s. When the robot is travelling under this speed, the optimal step length remains about 150 mm. When the robot is travelling above this speed, the step length changes according to the body velocity. But the cycle period changes very little.

This result can be applied in the design of the optimal gait parameters of the robot. When the robot is travelling lower than the critical speed, it is better to keep a constant stride length and change the cycle period. When the robot is travelling higher than this speed, it is better to keep a constant cycle period and change the stride length. By using this simplified method, the robot can choose the optimal parameters automatically to reduce the energy expenditure.

5 Simulations and Experiments on the Robot

In order to verify the theory, simulations and experiments of trotting with different gait parameters are carried out. The simulation software is called Recurdyn. It is a multi-body dynamic simulation software produced by FunctionBay.

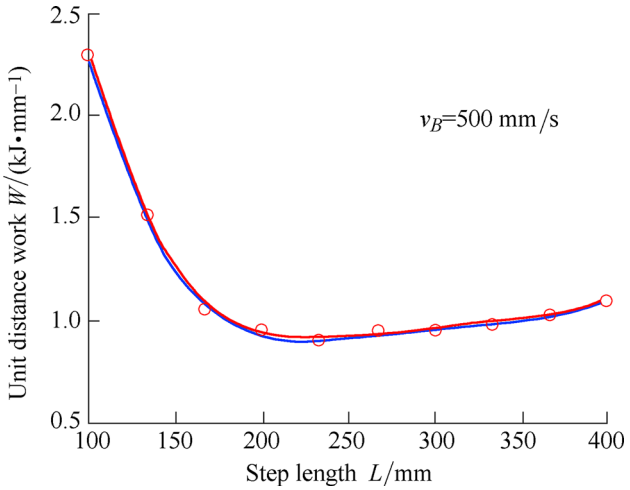

Fig. 13 Simulation results of the trotting gait

The mass of the model is 180 kg. The step height is 80 mm. The duty factor is 0.5. The robot walked 10 times with the same speed of 0.5 m/s. The step length in the body frame varies from 100 mm to 500 mm. The body displacement, the cylinder forces and the cylinder velocities were recorded. The power of the cylinders can be calculated. Figure 12 shows the simulation model.

By adding the mechanical work of all 12 cylinders together and dividing by the distance the robot travelled, the energy expenditure can be obtained. Figure 13 shows the energy expenditure recorded from simulations (curve with cycles) and its fitted curve (solid curve). It can be seen that there is a deviation between the simulation and the theory deduction due to the uncertainty of the impact forces and the touchdown moment. When the robot trotted with a smaller cycle period, the impact forces increased intensively in the simulations. However, there is clearly a certain step length that can minimize the energy expenditure of the robot.

Simulations were repeated on the real robot to verify the theory. The mass of the robot is also 180 kg. The robot trotted 10 times with different combinations of gait parameters. As shown in Fig. 14, force sensors and linear displacement sensors were configured on the actuators to measure the driving forces and positions.

Using the force data and the position data from the sensors, the power of the actuators can be calculated. By integrating the output power and dividing it by the distance the robot travelled, the energy expenditure of the robot can be estimated. The experiments of the trotting gait are shown in Fig. 15.

The energy expenditure curves are shown in Fig. 16. The circles represent the recorded experiment data and the

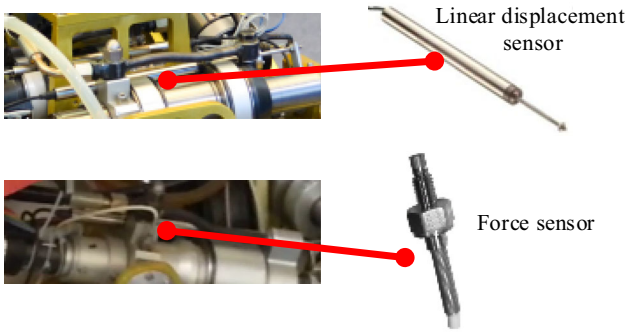

Fig. 14 Sensors on the robot

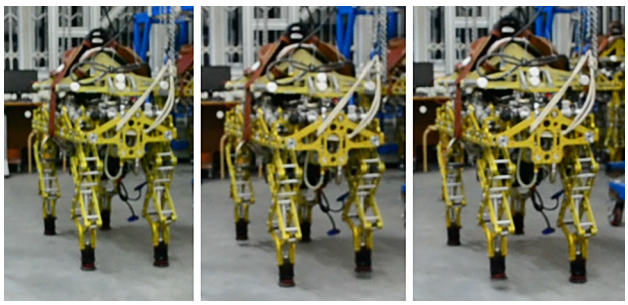

Fig. 15 Experiments of the trotting gait

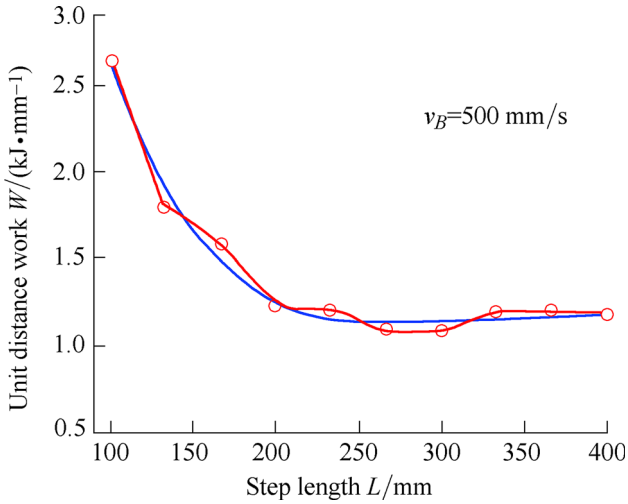

Fig. 16 Experiment results of the trotting gait

solid curve represents the fitted curve. The energy expenditures are larger compared to the simulations. This is due to the friction of the joints. However, the trend is very similar and the energy expenditure can be minimized.

Although the results from theory deduction, simulations and the experiments are not exactly the same, the trend is similar and clear. According to the data from the experiments, when the robot trots at 0.5 m/s using a 100 mm step length, the energy expenditure is about 2600 J/m. Comparing this to the energy expenditure 1200 J/m at the step length of 250 mm, an energy reduction of approximately 54% can be achieved. This improvement can make a substantial difference in the performance of the robot.

6 Conclusions

(1) The energy expenditure model of the quadruped robot is built. The analysis proves the existence of the optimal gait parameters that can minimize the energy expenditure.

(2) The critical trotting speed of the quadruped robot is found and the simplified gait parameter design approach is proposed to reduce the energy expenditure. When the robot is travelling lower than the critical speed, it is better to keep a constant stride length and change the cycle period. When the robot is travelling higher than this speed, it is better to keep a constant cycle period and change the stride length.

(3) During the experiments, the energy expenditure can be reduced by about 54% compared to the 100 mm stride length and 0.8 s cycle period under 500 mm/s speed.

References

1. RAIBERT M, BLANKESPOOR K, NELSON G, et al. Bigdog, the rough-terrain quadruped robot[C]//*Proceedings of the 17th World Congress, The International Federation of Automatic Control*, Seoul, July 6–11, 2008: 10823–10825.
2. SEMINI C, TSAGARAKIS N G, GUGLIELMINO E, et al. Design of HyQ—a hydraulically and electrically actuated quadruped robot[J]. *Proceedings of the Institution of Mechanical Engineers, Part I: Journal of Systems and Control Engineering*, 2011, 225(6): 831–849.
3. JIN H D, SEOK S, LEE J, et al. High speed trot-running: Implementation of a hierarchical controller using proprioceptive impedance control on the MIT Cheetah[J]. *The International Journal of Robotics Research*. 2014, 33(11): 1417–1445.
4. BOAVENTURA T, BUCHLI J, SEMINI C, et al. Model-Based hydraulic impedance control for dynamic robots[J]. *IEEE Transactions on Robotics*, 2015, 31(6): 1324–1336.
5. IQBAL J, TAHIR A M. Robotics for nuclear power plants–challenges and future perspectives[C]//*2012 2nd International Conference on Applied Robotics for the Power Industry*, Islamabad, Pakistan, September 11–13, 2012: 151–156.
6. MURPHY R R, TADOKORO S, NARDI D, et al. *Springer handbook of robotics*[M]. Berlin: Springer, 2008.
7. JUNYAO G, Wei B, JIANGUO Z. Coal mine detect and rescue robot design and research[C]//*IEEE International Conference on Networking, Sensing and Control*, Sanya, April 6–8, 2008: 780–785.
8. PAN Yang, GAO Feng, QI Chenkun, et al. Human-tracking strategies for a six-legged rescue robot based on distance and

view[J]. *Chinese Journal of Mechanical Engineering*. 2016, 29(2): 219–230.
9. XU Yilin, GAO Feng, PAN Yang, et al. Method for six-legged robot stepping on obstacles by indirect force estimation[J]. *Chinese Journal of Mechanical Engineering*. 2016, 29(4): 669–679.
10. FISCHER M, WERBER M, SCHWARTZ P V. Batteries: Higher energy density than gasoline[J]. *Energy policy,* 2009, 37(7): 2639–2641.
11. MADDEN J D. Mobile robots: motor challenges and materials solutions[J]. *Science*, 2007, 318(5853): 1094–1097.
12. ALEXANDER R M. Three uses for springs in legged locomotion[J]. *The International Journal of Robotics Research*, 1990, 9(2): 53–61.
13. LAFFRANCHI M, TSAGARAKIS N G, CANNELLA F, et al. Antagonistic and series elastic actuators: a comparative analysis on the energy consumption[C]//*IEEE/RSJ International Conference on Intelligent Robots and Systems*, Louis, October 11–15, 2009: 5678–5684.
14. GREGORIO P, AHMADI M, BUEHLER M. Design, control, and energetics of an electrically actuated legged robot[J]. *IEEE Transactions on Systems, Man, and Cybernetics, Part B: Cybernetics,* 1997, 27(4): 626– 634.
15. ACKERMAN J, SEIPEL J. Energy efficiency of legged robot locomotion with elastically suspended loads[J]. *IEEE Transactions on Robotics*, 2013, 29(2): 321–330.
16. CHEN Xianbao, GAO Feng, Qi Chenkun, et al. Spring Parameters Design for the New Hydraulic Actuated Quadruped Robot [J]. *Journal of Mechanism and Robotic*, 2014, 6(2): 021003.
17. ALEXANDER R M. Energy-saving mechanisms in walking and running[J]. *Journal of Experimental Biology*, 1991, 160(1): 55–69.
18. HOYT D F, WICKLER S J, COGGER E A. Time of contact and step length: the effect of limb length, running speed, load carrying and incline[J]. *Journal of Experimental Biology*, 2000, 203(2): 221–227.
19. HOYT D F, WICKLER S J, DUTTO D J, et al. What are the relations between mechanics, gait parameters, and energetics in terrestrial locomotion[J]. *Journal of Experimental Zoology Part A: Comparative Experimental Biology*, 2006, 305(11): 912–922.
20. MINETTI A, ARDIGO L, REINACH E, et al. The relationship between mechanical work and energy expenditure of locomotion in horses[J]. *Journal of Experimental Biology*, 1999, 202(17): 2329–2338.
21. CAVAGNA G A, FRANZETTI P, HEGLUND N C, et al. The determinants of the step frequency in running, trotting and hopping in man and other vertebrates[J]. *The Journal of Physiology*, 1988, 399(1): 81–92.
22. HOLT K G, HAMILL J, ANDRES R O. Predicting the minimal energy costs of human walking[J]. *Medicine and Science in Sports and Exercise*, 1991, 23(4): 491–498.
23. HOLT K G, JENG S F, RATCLIFFE R, et al. Energetic cost and stability during human walking at the preferred stride frequency[J]. *Journal of Motor Behavior*, 1995, 27(2): 164–178.
24. AHLBORN B K, BLAKE R W. Walking and running at resonance[J]. *Zoology*, 2002, 105(2): 165–174.
25. ZHANG Jiaqi, GAO Feng, HAN Xiaolei, et al. Trot gait design and CPG method for a quadruped robot[J]. *Journal of Bionic Engineering,* 2014, 11(1): 18–25.
26. CHEN Xianbao, GAO Feng, QI Chenkun, et al. Spring parameters design to increase the loading capability of a hydraulic quadruped robot[C]//*IEEE International Conference on Advanced Mechatronic Systems,* Luoyang, September 25–27, 2013: 535–540.
27. CHEN Xianbao, GAO Feng, QI Chenkun, et al. Gait planning for a quadruped robot with one faulty actuator[J]. *Chinese Journal of Mechanical Engineering*, 2015: 1–9.
28. GAO Feng, QI Chenkun, SUN Qiao, et al. A quadruped robot with parallel mechanism legs[C]//*IEEE International Conference on Robotics and Automation (ICRA),* Hong Kong, June 1–5, 2014: 2566–2566.

Xian-Bao Chen, born in 1981, is currently a Post doctor at *State Key Laboratory of Mechanical System and Vibration, Shanghai Jiao Tong University, China*. His research interests include parallel mechanism and legged robots. E-mail: xianbao@sjtu.edu.cn

Feng Gao, born in 1956, is currently a professor at *Shanghai Jiao Tong University, China*. His main research interests include parallel robots, design theory and its applications, large scale and heavy payload manipulator design, large scale press machine design and optimization, design and manufactory of nuclear power equipment, legged robots design and control. E-mail: fengg@sjtu.edu.cn